

# Electrochemically polymerized composites of conducting poly(*p*-ABSAs) and flavins (FAD, FMN, RF) films and their use as electrochemical sensors: A new potent electroanalysis of NADH and NAD<sup>+</sup>

S. Ashok Kumar, Shen-Ming Chen \*

*Department of Chemical Engineering and Biotechnology, National Taipei University of Technology, No. 1, Section 3, Chung-Hsiao East Road, Taipei 106, Taiwan, ROC*

Received 10 August 2006; received in revised form 16 October 2006; accepted 31 October 2006  
Available online 13 December 2006

## Abstract

We report the preparation and characterization of poly(*p*-aminobenzene sulfonic acid) (PABS) films doped with flavins (flavin adenine dinucleotide (FAD), flavin mononucleotide (FMN), riboflavin (RF)). It is noted as PABS/flavins modified electrodes. In this study, the conducting polymer, PABS served as a matrix during the electropolymerization to synthesize PABS/flavin composite films. The synthetic, morphological and electrochemical properties of PABS/flavin films and PABS films were compared. Characterization was performed by cyclic voltammetry (CV), atomic force microscopy (AFM), scanning electron microscopy (SEM) and ultraviolet visible (UV–vis) spectroscopy. AFM and SEM images revealed that the incorporation of flavins significantly altered the morphology of the PABS films. UV–vis spectroscopy confirmed the presence of flavins within composite films. PABS/FAD composite modified glassy carbon electrode (PABS/FAD/GCE) is used to electrochemically detect NADH and NAD<sup>+</sup>. PABS/FAD/GCE showed excellent electrocatalytic activity for the oxidation of NADH and for the reduction of NAD<sup>+</sup>. At optimum conditions, the sensor has a fast response to NADH and a good linear response observed for NADH in the range from 10 to 300 μM. The cyclic voltammograms (CVs) waves of nicotinamide adenine dinucleotide reduction-oxidation (NAD<sup>+</sup>/NADH) reversible reaction was also observed. © 2006 Elsevier B.V. All rights reserved.

**Keywords:** Polymer composite; Flavins; Modified electrodes; NADH oxidation; NAD<sup>+</sup> reduction; Sulfanilic acid

## 1. Introduction

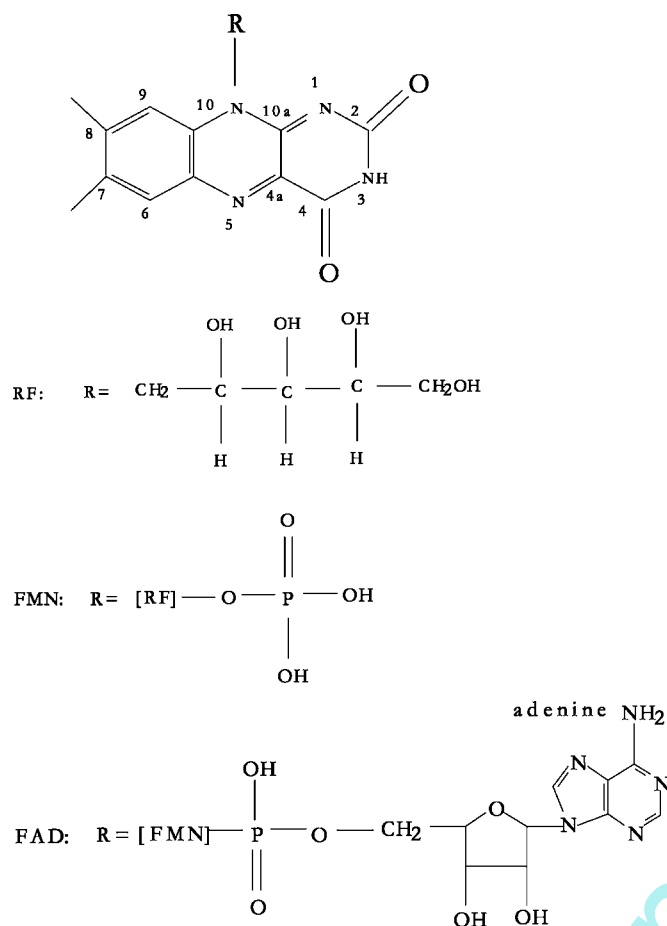
The flavins are an important class of biochemical compounds which are found in both plants and animals. Due to their importance, most of the flavins have been the subject of many studies. In particular isoalloxazine, riboflavin, and flavin mononucleotide have been thoroughly investigated and excellent reviews of these studies are available [1]. Flavin adenine dinucleotide (Scheme 1) occupies a key position in the respiratory transport chain [1]. The electrochemical reaction mechanism of FAD was thoroughly studied on various electrode materials by many authors throughout a broad pH range in aqueous solution [1–5].

One of the simplest methods of immobilizing biomolecules on polymer surfaces is adsorption [6]. This includes both phys-

ical adsorption and electrochemical adsorption techniques. The latter is achieved by applying a potential to the polymer electrode surface, which enhances electrostatic interactions and hence immobilization [7]. The main disadvantage of adsorption, however, is that the biomolecule may easily desorb from the surface during use.

Covalent attachment of biomolecules to the surface of polymers ensures immobilization without leaching of the biomolecule from the substrate surface [8]. Covalent attachment of biomolecules to the monomer prior to polymerization has also been reported [9,10]. This strategy, however, requires lengthy syntheses to produce the monomer or to modify a preformed surface. Because covalent attachment is usually achieved using a linker, the separation of the biomolecule from the polymer backbone can also have disadvantages in terms of signal transduction [11]. Self-assembly techniques have been investigated for biomolecule immobilization onto various support materials. Layers formed by self-assembly require a polyion to effect biomolecule attachment through strong electrostatic interaction

\* Corresponding author. Tel.: +886 2 27017147; fax: +886 2 27025238.  
E-mail address: [smchen78@ms15.hinet.net](mailto:smchen78@ms15.hinet.net) (S.-M. Chen).



Scheme 1. Oxidized form of the isoalloxazine ring system and members of the flavin family, as defined by the nature of the **R** group attached to N-10.

[12–14] and can result in tightly packed structures that limit diffusion [15]. Furthermore, careful control of pH is required to achieve these assemblies and for them to retain stability.

Biomolecules have been trapped within conducting polymers as dopant molecules when the appropriate conditions are met [16,17]. To function as a dopant for oxidized conducting polymers, anions are required. The vapor phase polymerization of polypyrrole, poly-terthiophene and poly-3,4-ethylenedioxy thiophene has been reported, which allows the incorporation of biomolecules (guest) within the polymer matrix via a simple washing step [18–20].

Among electrically conducting polymers, polyaniline and its derivatives have been the focus of much attention. Sulfonated polyaniline (SPAN) is of interest because of its unusual physical properties, improved processability, and potential industrial applications [21–26]. SPAN is the first reported self-doped water-soluble conducting polyaniline derivative and a prime model for dopant and secondary dopant-induced processability [27,28]. The solubility of polyaniline in aqueous solutions and in most common organic solvents is greatly improved by the presence of  $-\text{SO}_3^-$  groups [29]. The environmental stability of the parent polyaniline is also further improved in SPAN. The conductivity of SPAN is independent of external protonation in a broad pH range. SPAN was found to have better thermal stability than its parent polyaniline [30].

On other hand, nicotinamide adenine dinucleotide (phosphate) ( $\text{NAD(P)}^+/\text{NAD(P)H}$ ) dependent enzymes, which trivially called dehydrogenases, constitute the largest group of the enzymes known nowadays. The number of characterized dehydrogenases is more than 500. These enzymes use the turnover of nicotinamide adenine dinucleotide as a coupled redox reaction. Electrochemical regeneration of this cofactor is extremely important from both fundamental and practical points of view. Biotechnological applications of this reaction include the development of the biosensors for a great number of analytes, the biofuel cells with different cheap fuels and would provide the stereo-specific electrosynthesis of organic compounds [31].

Due to continuous efforts of bioelectrochemists during last three decades, the mediators for ( $\text{NAD}^+/\text{NADH}$ ) regeneration have been proposed. Quinones [32,33] and phenoxazine derivatives containing quinoid structures [34,35] and polyaniline [36] have been used successfully as two-electron catalysts for NADH oxidation. Several phenoxazines transferring one proton per two electrons have also been found to be suitable mediators of pyridine nucleotide electrooxidation [37,38]. On the contrary, the only mediator found for  $\text{NAD}^+$  electroreduction was the rhodium (III)-bipyridyl complex [39]. However, all these systems required sufficient over voltages and were not able to catalyze both  $\text{NAD}^+$  reduction and NADH oxidation. Moreover, the use of diffusion-free mediators for  $\text{NAD}^+/\text{NADH}$  regeneration was not plausible especially in analytical applications, because the resulting systems are operated with the two diffusion-free mediators including  $\text{NAD}^+/\text{NADH}$  itself. Recently, our research group has been reported the new electrocatalyst based on FAD incorporated modified electrode for  $\text{NAD}^+/\text{NADH}$  reversible reaction [40–42].

In this paper, we report the new polymer composite material electrochemically synthesized by using *p*-aminobenzene sulfonic acid (*p*-ABSA) and flavins on glassy carbon electrodes (GCE) and indium tin oxide coated (ITO) glass electrodes. We found that the adsorption of flavins occurs in the order of  $\text{RF} < \text{FMN} < \text{FAD}$  on the polymer materials. We observed this modified electrode very stable in the pH ranges between 2 and 10, with well separated two redox waves. Here we demonstrate that the new potent electrode material for electrocatalytic oxidation of NADH and for electrocatalytic reduction of  $\text{NAD}^+$ . Furthermore, the  $\text{NAD}^+/\text{NADH}$  reversible reaction was also observed at physiological condition. Indeed, when compared to other reported electrode materials by other groups [31] and ourselves [40–42], this new polymer composite material as an opted electrode material for electroanalysis of NADH and  $\text{NAD}^+$ .

## 2. Experimental

### 2.1. Reagents and equipment

All chemicals and reagents used in this work were of analytical grade, and were used as received without further purification. These were: flavin adenine dinucleotide disodium salt (97%), flavin mononucleotide (95%) and riboflavin (98%),  $\beta$ -nicotinamide adenine dinucleotide reduced form (98%),  $\beta$ -nicotinamide adenine dinucleotide (98%), and

*p*-aminobenzenesulfonic acid were purchased from Sigma chemical company, USA. Supporting electrolytes used for electrochemical experiments were 0.1 M H<sub>2</sub>SO<sub>4</sub>, 0.1 M HNO<sub>3</sub>, 0.2 M phosphate and 0.1 M acetate buffer solutions. The aqueous solutions were prepared by using doubly distilled deionized water, and before each experiment the solutions were deoxygenated by purging with pre-purified nitrogen gas.

Electrochemical measurements were performed with CH Instruments Model-1200A with conventional three-electrode cell. A BAS glassy carbon and platinum wire are used as the working electrode and counter electrode, respectively. All the cell potentials were measured with respect to an Ag/AgCl [KCl (sat)], reference electrode. HITACHI Model S-3000H scanning electron microscope was used for surface image measurements. The UV–vis absorption spectra were checked by using a U3300 Spectrophotometer (HITACHI). The AFM images were recorded with a Multimode Scanning Probe Microscope System operated in tapping mode, (CSPM4000, Ben Yuan Ltd.). All experiments were carried out at room temperature.

## 2.2. Synthesis of PABS/flavin and PABS films

Prior to use, the working electrodes were mechanically polished with alumina powder (Al<sub>2</sub>O<sub>3</sub>, 0.05 μm) up to a mirror finish. Then the electrodes were cycled in 0.2 M sulfuric acid in a potential range –0.5 to 1 V at a sweep rate of 100 mV s<sup>–1</sup> until a stable voltammogram obtained. The electrochemical deposition of PABS/flavin films was carried out by cyclic voltammetry (between –0.5 and 2.0 V at 100 mV s<sup>–1</sup>) for 30 cycles or potentiostatically by applying a potential at 2 V for 20 min. The electropolymerization was conducted in a three-electrode cell with glassy carbon as the working electrode, Ag/AgCl as the reference electrode and platinum wire as the counter electrode. The electrolyte consisted of 2 mM *p*-aminobenzenesulfonic acid monomer and 1 mM FAD or 1 mM FMN or 1 mM RF in aqueous solution of 0.1 M HNO<sub>3</sub>. The resulting films were washed with doubly distilled deionized water before analysis. For comparison, PABS films were prepared under the same experimental conditions using aqueous solution of 0.1 M HNO<sub>3</sub>, in the absence of flavin molecules. Finally, the modified GCE was electroactivated by cyclic voltammetry from –0.75 to 0.65 V in pH 6.4 phosphate buffer solution (PBS) at a scan rate of 100 mV s<sup>–1</sup>.

## 3. Results and discussion

### 3.1. Electrochemical synthesis of PABS/FAD and PABS films

Fig. 1A shows the growth of PABS/FAD films onto a GCE. Since the FAD molecules and NO<sub>3</sub><sup>–</sup> were the only species in solution other than *p*-ABSA in the formation of PABS/FAD film, this implied that the FAD acted as dopant as indicated by an increase in current with electrolysis time and the formation of a yellow coating was observed on electrode surface. Furthermore, in the absence of FAD molecules in the electrolyte medium the growth of the blue polymer coating was observed,

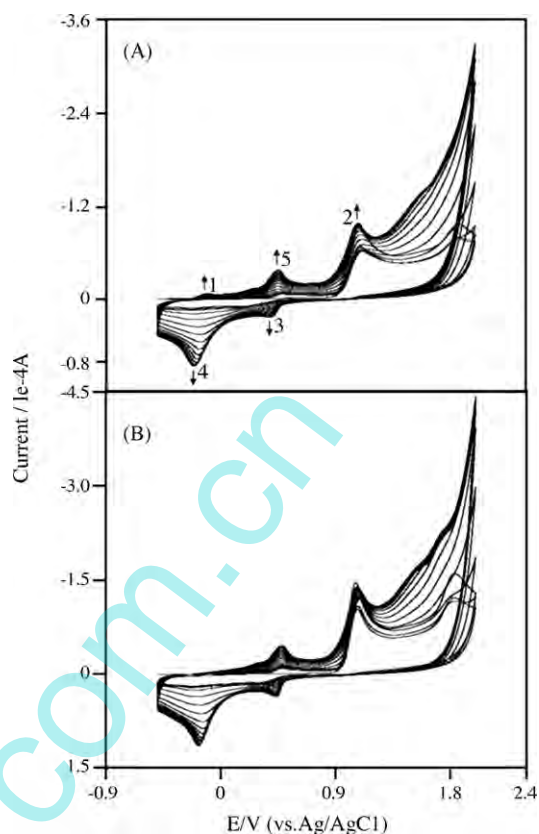
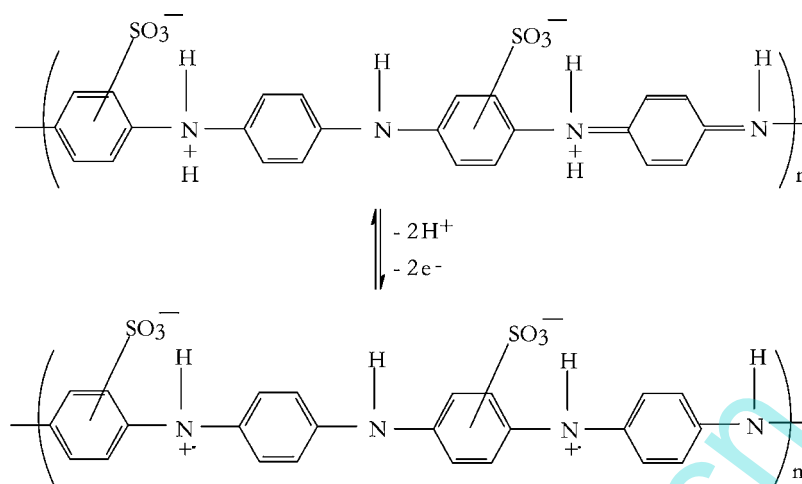


Fig. 1. (A) CVs of the film growth of PABS/FAD on GCE from electrolyte 0.1 M HNO<sub>3</sub> solution containing 2 mM *p*-ABSA and 1 mM FAD (pH 2.0). (B) CVs of the film growth of PABS on GCE from 0.1 M HNO<sub>3</sub> solution containing 2 mM *p*-ABSA. Scan rate = 0.1 V s<sup>–1</sup>.

demonstrating that FAD molecules indeed incorporated in the polymerization. There is no adsorption of FAD molecules on GCE [5] was observed during electrochemical cycling in the potential range used for polymerization in the absence of *p*-ABSA. This is additional evidence that FAD acted as a dopant in the electropolymerization process.

Further, Fig. 1A shows, in the first scan, anodic peaks 1 and 2 were observed with peak potential value at –0.12 and 1.11 V, respectively. From the second scan on, cathodic peaks 3 and 4 were observed with peak potential value at 0.39 and –0.18 V. From the second cycle anodic peak 5 appeared with potential at 0.45 V. Then larger peaks were observed upon continuous scanning, reflecting the continuous growth of the film. These facts indicated PABS/FAD film was deposited on the surface of GCE by electropolymerization. A uniform adherent yellow polymer film was formed on the GCE surface. For comparison, PABS films were prepared under the same conditions using aqueous solution of 0.1 M HNO<sub>3</sub>, in the absence of FAD molecules. After modification, the PABS/FAD and PABS film electrodes were carefully rinsed with doubly distilled water, then stored in air and used for analysis.

The electrochemical polymerization mechanism of *p*-ABSA at GCE was similar to the references reported [43]. The reaction mechanism may be described as follows *p*-ABSA was first oxidized to free radical (peak 2); the free radical combined together rapidly to hydrazobenzene sulfonic acid; then hydrazobenzene



Scheme 2. The electrochemical process of PABS polymer peak.

sulfonic acid was oxidized to azobenzene sulfonic acid (peak 5), and azobenzene sulfonic acid reduced to hydrazobenzene sulfonic acid (peak 3).

In the confirmed mechanism of polyaniline formation, the cation radical, which is primarily formed as the product of the electrooxidation, loses a proton forming a neutral species. The latter dimerizes with another cation radical. As a result of further electrooxidations and proton losses followed by the attacks of the cation radicals, trimers, oligomers, and eventually polyaniline are formed [21,23]. During the formation of PABS, the primary species is the cation radical of *p*-ABSA formed during the electrolysis as suggested in [21]. The copolymers of aniline and aniline sulfonic acids are produced with the attack of either the aniline cation radical or the cation radical of aniline sulfonic acids on the intermediate neutral species. Incorporation of aniline sulfonic acid units into the polymer chain prevents the autocatalytic growth of polyaniline, producing less conductive lower molecular weight polymers [23]. Cyclic voltammograms of polymer redox process of azobenzene sulfonic (peak 5) acid to hydrazobenzene sulfonic acid (peak 3) was given in Scheme 2.

The developing of anodic peak (1) and cathodic peak (4) in the CVs of Fig. 1A shows the co-deposition of FAD molecules within polymeric film onto the GCE surface. Fig. 1B shows the formation of PABS films in the absence of FAD molecules in the electrolyte solution, two anodic peak (peaks 2 and 5) and one cathodic peak (peak 3) were observed, the blue color polymer was obtained on GCE as mentioned earlier [23]. For comparison, PABS modified GCE was prepared and its electrochemical behaviors was tested. A reduction peak (peak 4) in Fig. 1A and 1B centered at  $-0.12$  V may due to the insertion of anions (for example  $\text{NO}_3^-$  and  $\text{SO}_4^{2-}$ ) accompanied by the hydrogenation of polymer site [21,23], this cathodic peak was overlap with reduction peak of FAD during synthesis of PABS/FAD film.

### 3.2. Electrochemical behavior of PABS/FAD and PABS film modified GCEs

Fig. 2 shows a comparison of the CVs of the PABS/FAD and PABS film modified GCE in pH 6.4 PBS reveals that the currents

attained in the both case are almost equal, due to the entrapment of the FAD molecules in the polymer backbone additional redox wave was obtained for PABS/FAD/GCE, the formal potentials ( $E^0$ ) ( $E_{pc} + E_{pa}/2$ ) are  $-0.4$  and  $0.07$  V for FAD and PABS at pH 6.4 (Fig. 2a), respectively. PABS modified GCE was shown only one redox wave centered at  $0.09$  V (Fig. 2b) when compared to PABS/FAD/GCE,  $20$  mV difference are observed in  $E^0$  value for polymer redox waves, this potential difference may arise due to the adsorption of FAD molecules onto the polymer backbone. To ascertain the solution behavior of FAD in pH 6.4 PBS, the CV was recorded in the buffer solution containing  $1$  mM FAD by using well cleaned bare GCE, Fig. 2a and 2c shows cyclic voltammograms of PABS/FAD/GC and the redox waves of  $1$  mM FAD recorded at a scan rate of  $100$  mV s $^{-1}$ . A pair of small redox peaks can be seen for the FAD at bare GCE,  $E^0$  is  $-0.38$  V, which is in good agreement with a literature report [5]. For the PABS/FAD/GC films shows a pair of well defined redox peaks can be seen at  $-0.4$  V ( $E^0$ ) versus Ag/AgCl, attributed to the oxidation and reduction of isoalloxazine group of FAD. Note that the currents obtained for PABS/FAD/GCE was one

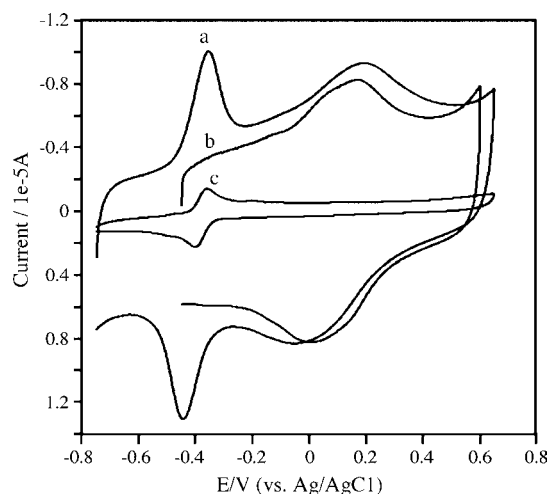


Fig. 2. CVs of (a) PABS/FAD, (b) PABS films modified GCE in pH 6.4 PBS and (c) CV of  $1$  mM FAD in pH 6.4 PBS at bare GCE. Scan rate =  $0.1$  V s $^{-1}$ .

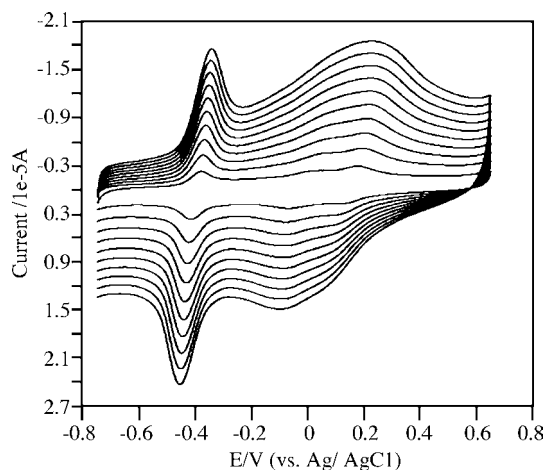


Fig. 3. CVs of PABS/FAD/GCE in pH 6.4 PBS at different scan rates. The scan rates from inner to outer are 0.02, 0.04, 0.06, 0.08, 0.10, 0.12, 0.14, 0.16, 0.18, and 0.20  $\text{V s}^{-1}$ , respectively.

order of magnitude higher than that obtainable for the FAD in solution at GCE; it was clearly shown the advantages of using the polymer PABS as a matrix for immobilization of FAD are evident, since a large surface area is available.

Fig. 3 shows the cyclic voltammograms of the PABS/FAD/GCE by immersing in pH 6.4 PBS at different scan rates in potential range  $-0.75$  to  $0.65$  V. As shown in Fig. 4A and 4B the peak currents increased linearly with the scan rate between 10 and  $100 \text{ mV s}^{-1}$  as expected for a surface process. Moreover, the anodic peak currents were almost the same as the corresponding cathodic peak currents and the peak potential did not change with increasing the scan rate. The peak-to-peak potential separation ( $\Delta E_p = \Delta E_{pa} - \Delta E_{pc}$ ) is about 30 and 160 mV for FAD and polymers redox peaks were obtained at sweep rates below  $100 \text{ mV s}^{-1}$ , suggesting facile charge transfer kinetics over this range of sweep rate. At higher sweep rates, the plot of peak currents versus scan rate deviates from linearity and the peak current becomes proportional to the square root of the scan rate (Fig. 4A and 4B), indicating a diffusion controlled process, which is reflective of the relatively slow diffusion of counter ions into the electrode surfaces. At higher sweep rates ( $\nu > 100 \text{ mV s}^{-1}$ ) peak separations begin to increase, indicating the limitation due to charge transfer kinetics. Based on Laviron theory [44] the electron transfer rate constant ( $K_s$ ) and charge transfer coefficient ( $\alpha$ ) can be determined by measuring the variation of peak potential with scan rate. The values of peak potentials were proportional to the logarithm of the scan rate for scan rates higher than  $2.0 \text{ V s}^{-1}$  (Fig. 5). The slope of the  $\Delta E_{pc}$  versus  $\log(\nu)$  was about 191 mV for FAD and was about 275 mV for polymer peak. Using the equation  $E_p = K - 2.3030(RT/\alpha nF) \log(\nu)$  and the two electrons transferred for FAD a charge transfer coefficient ( $\alpha$ ) 0.48 was obtained. Introducing these values in the equation [45]:

$$\log K_s = \alpha \log(1 - \alpha) + (1 - \alpha) \log \alpha - \log(RT/nF\nu) - \alpha(1 - \alpha)nFE/2.3RT \quad (1)$$

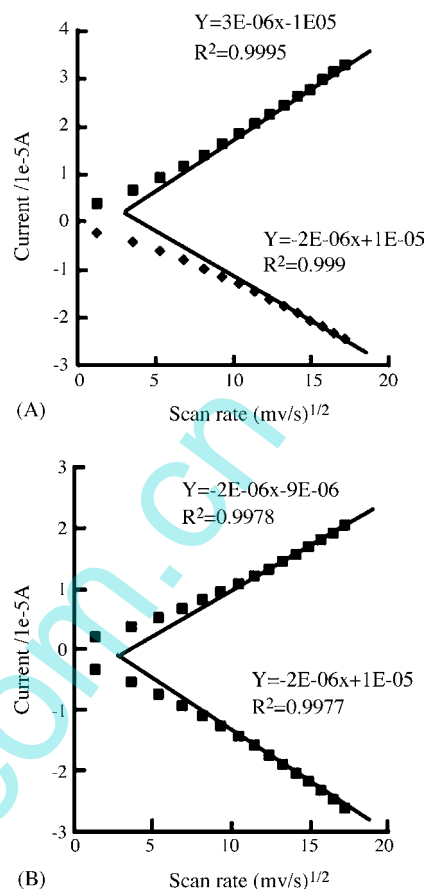


Fig. 4. (A) Plot of FAD peak currents vs. square root of scan rate and (B) plot of polymer peak currents vs. square root of scan rate.

An apparent surface electron transfer rate constant ( $K_s$ )  $187 (\pm 5) \text{ s}^{-1}$ , was estimated for reversible redox waves of FAD in PABS/FAD/GCE. This larger value of electron transfer rate constant indicate high ability of PABS for promote electron between FAD and electrode surface.

For comparison, in the same manner, the electrochemical synthesis of PABS/FMN and PABS/RF were prepared on GC electrodes from the electrolyte containing 1 mM FMN or RF and *p*-ABSA in 0.1 M  $\text{HNO}_3$ . Fig. 6a and 6b shows the cyclic voltammogram of PABS/RF and PABS/FMN modified GC electrodes in pH 6.4 PBS. The surface coverage concentration ( $\Gamma$ ) of FAD, FMN, and RF were evaluated from the following equation:

$$\Gamma = \frac{Q}{nFA} \quad (2)$$

where  $A$  ( $=0.0707 \text{ cm}^2$ ) is the area of the glassy carbon electrodes,  $n$  ( $=2$ ) the number of electrons per reactant molecule,  $Q$  the charge obtained by integrating the anodic peak at low voltage scan rate ( $20 \text{ mV s}^{-1}$ ), and  $F$  is the Faraday constant. We assume that all of the immobilised redox centers are electroactive on the voltammetry time scale. In the present case, the calculated values of  $\Gamma$ ,  $E^0$ ,  $\Delta E_p$ , for PABS/FAD, PABS/FMN, and PABS/RF modified GC electrodes are presented in Table 1.

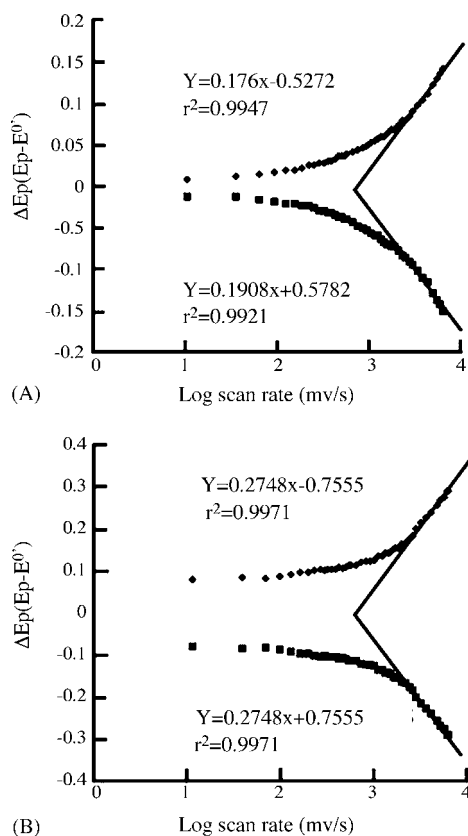


Fig. 5. Plot of peak potential separation vs.  $\log v$  for GCE modified with PABS/FAD: (A) FAD redox peak and (B) polymer peak, respectively.

### 3.3. Stability and pH dependence of the PABS/FAD, PABS/FMN and PABS/RF modified GC electrodes

The stability of the PABS/FAD/GCE and the reproducibility of the electrochemical behavior were investigated by cyclic voltammetry. Under continuous potential sweeping at  $100 \text{ mV s}^{-1}$  between 0.7 and  $-0.65 \text{ V}$  in 0.1 M phosphate buffer solution (pH 6.4), an insignificant decay in the peak currents was observed during the initial cycles (1% for first 25 cycles), and the rate of current decrease then decreased (4% after 200 cycles) (Fig. 7A). In addition it was found that the current only decreased by 5% when the electrode was immersed in buffer solution (pH 6.4) for 30 h. The stability of the modified electrodes was evaluated by the same method in electrolyte solutions with pH 2 and 10. The results indicated the modified electrode was stable at acidic solution, but in alkaline media (pH 10) more decrease was observed in the peak currents (10% after 100 cycles). These results suggest that the initial decay might be due to material that is weakly bonded to the electrode surface. Since the method of

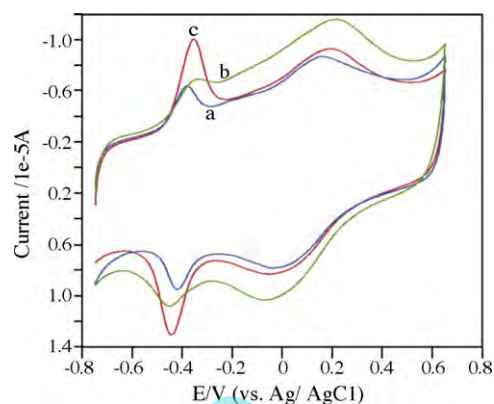


Fig. 6. CVs of (a) PABS/RF and (b) PABS/FMN and (c) PABS/FAD films modified GCE in pH 6.4 PBS. Scan rate =  $0.1 \text{ V s}^{-1}$ .

the electrode preparation is simple and fast (less than 20 min), the current decay is not a serious limitation for this modified electrode.

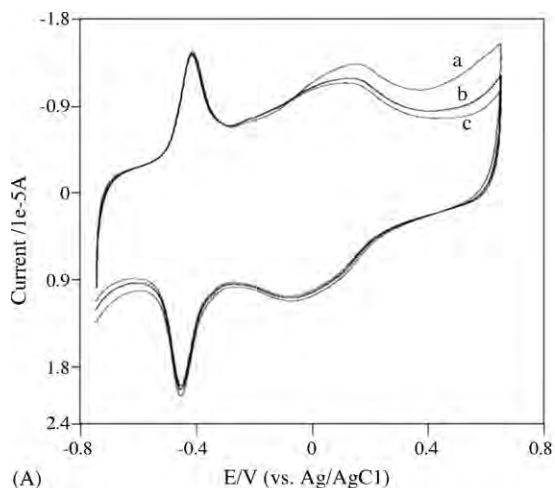
On other hand, the stability of the PABS/FMN and PABS/RF modified GC electrode and the reproducibility of the electrochemical behavior were also investigated by cyclic voltammetry in the procedure used for PABS/FAD/GCE. An insignificant decay in the peak currents was observed during the initial cycles (2% for first 25 cycles), and the rate of current decrease then decreased (10% after 200 cycles). In addition it was found that the current decreased by 10% when the electrode was immersed in buffer solution (pH 6.4) for 30 h. Indeed, when compared to PABS/FAD/GCE, the rate of current decrease is higher for PABS/FMN and PABS/RF modified GCEs, this indicating the interaction of FMN and RF are not enough stronger on the polymeric film than FAD molecules. Note that the  $\Gamma$  value of FAD is higher than FMN and RF modified electrodes (Table 1), this is another evident for stronger interaction between FAD molecules and PABS film (see Fig. 6).

It has been shown that FAD adsorbs very strongly in two different orientations on a mercury electrode surface in neutral solutions. At dilute coverages, it has been suggested that both the isoalloxazine and adenine moieties are adsorbed parallel to the electrode surface at all potentials, while at higher surface coverages, FAD can reorient to a perpendicular configuration [46,47], particularly at potentials near the pzc. In acidic solutions [2,48], evidence for a third tightly packed orientation has been obtained, in which the adenine group, now protonated, is no longer on the electrode surface, resulting in improved lateral interactions and tighter packing of adjacent isoalloxazine ring systems. The adsorbed FAD monolayer is believed to reorient, concertedly, between parallel and perpendicular, as the potential is changed in all solutions.

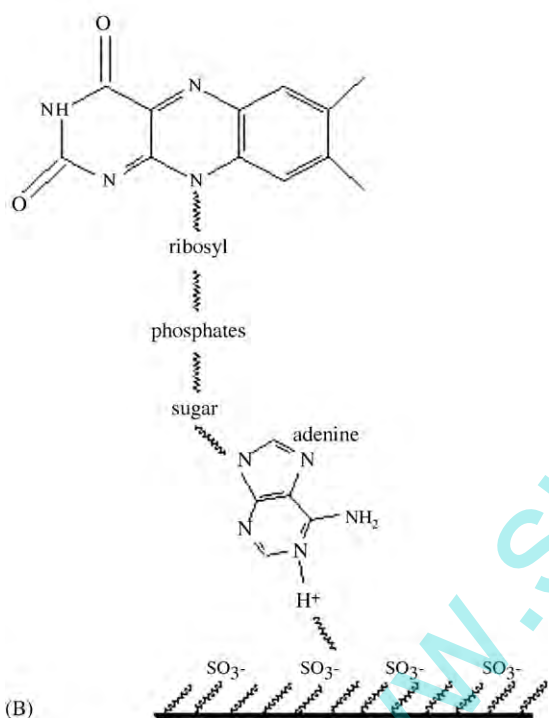
Table 1

Formal potentials and surface coverage for FAD, FMN, and RF on the PABS/FAD, PABS/FMN, and PABS/RF modified GC electrodes

Modified GCEs	$E_{pa}$ (V)	$E_{pc}$ (V)	$\Delta E_p$ (mV)	$E^0$ (V)	$\Gamma$ ( $\times 10^{-10} \text{ mol cm}^{-2}$ )
PABS/FAD	-0.390	-0.408	18	-0.399	6.2154
PABS/FMN	-0.393	-0.419	26	-0.406	5.3211
PABS/RF	-0.395	-0.419	24	-0.407	5.0063



(A)

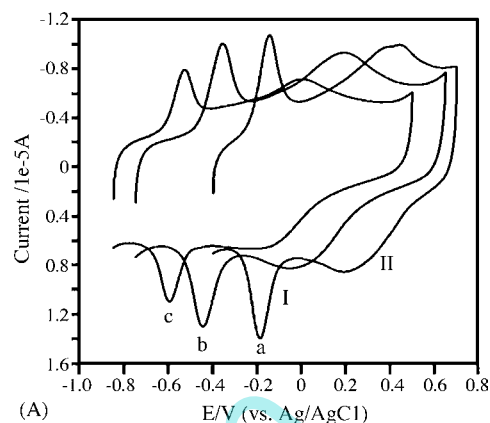


(B)

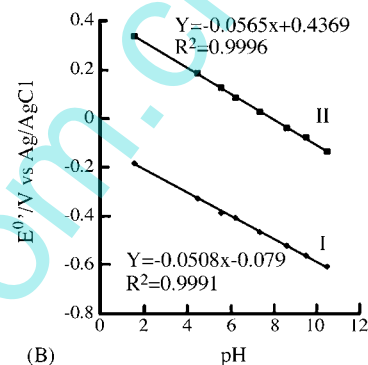
Fig. 7. (A) CVs of PABS/FAD/GCE in phosphate buffer solution: (a) 1st cycle, (b) 100th cycle and (c) 200th cycle. (B) Schematic diagram of adsorption of FAD molecules with PABS films.

The distinctive electrochemistry of FAD at pH less than ca. 4.5 indicates that the adenine group of FAD has a  $pK_a$ , of ca. 4.5–5 [2,48]. In our experimental condition (pH 2) adenine moiety is positively charged and it is reasonable that this interaction would be more stable at the negative end of the dipole of the isoalloxazine system and the positively charged adenine group is now pointed directly towards the negatively charged polymer (PABS) modified electrode surface. The schematic representation of interaction between adenine and negatively charged polymer are presented in Fig. 7B.

Recently the comparative study of immobilization of FAD, FMN, and RF on silica gel modified with zirconium oxide (Si:Zr) was reported [49], the flavins were strongly adsorbed on these materials, the higher amount of adsorbed FMN and FAD can



(A)



(B)

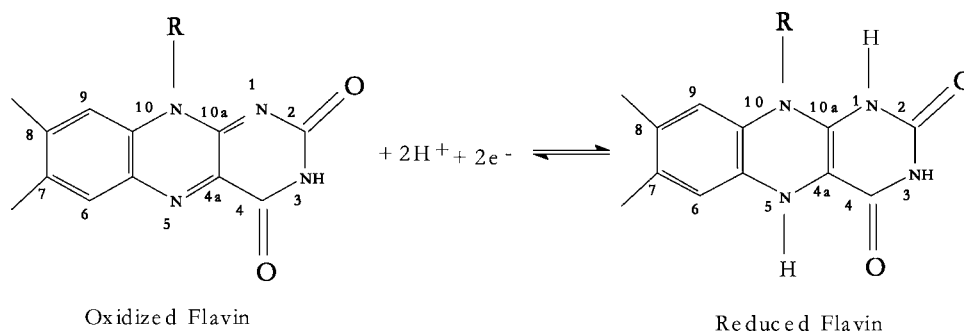
Fig. 8. (A) CVs for PABS/FAD/GCE at different pH values: (a) 2.2, (b) 6.4 and (c) 10.2. Scan rate  $0.1 \text{ V s}^{-1}$ . (B) Formal potentials as a function of pH at scan rate of  $0.1 \text{ V s}^{-1}$ .

be attributed to the large affinity of zirconium to the phosphate group present in flavin structure. However, other types of interaction must also be involved, since RF, which does not have a phosphate group, was also adsorbed on Si:Zr, they are suggested the interaction between Si:Zr and RF should occur via the isoalloxazine ring [49] so, the adsorption of FMN and RF occurred with PABS by different interactions [2,49].

The effect of pH on the PABS/FAD, PABS/FMN and PABS/RF-modified GCEs signal were investigated by recording cyclic voltammograms using  $0.1 \text{ M}$  PBS at various pH values from 2 to 11 (Fig. 8A). As can be seen in Fig. 8B, the formal potential of the both surface redox couple was pH dependent. A plot of  $E^{0'}$  versus pH gives a straight line from pH 2 to 11 for PABS/FAD, PABS/FMN, and PABS/RF modified GCEs. The results are presented in Table 2. These values are very close to the anticipated Nernstian value of  $59 \text{ mV}$  for a two-electron–two-proton process (Scheme 3). The value obtained for the slopes of surface deposited flavins is much closed to that reported in literature [50].

Table 2  
The slope values of the plot of  $E^{0'}$  vs. pH of the modified electrodes

Modified electrodes	Slopes (mV/pH)
PABS/FAD	50.8
PABS/FMN	49.8
PABS/RF	50.8



Scheme 3. Redox process of part of the flavin (isalloxazine ring) structure.

### 3.4. Surface characterization of PABS/FAD and PABS films

The surface morphology of the films was characterized by SEM and AFM. As shown in Fig. 9, the surface morphology of PABS/FAD film was significantly different from that of PABS film. As previously reported by other researchers for polyaniline [51] and as illustrated in Fig. 9B, a highly porous material is obtained for a PABS film grown, 0.3–0.1 μm holes are seen on the PABS film structures. However, even if the roughness and the porosity are similar to that obtained for PANI electropolymerized from an aqueous media [51], some morphological differences were observed. Indeed, a grainy structure was

found for PABS/FAD films (Fig. 9A), and also micro-holes on the PABS film was fully covered by the flavins.

Fig. 10 shows the morphology (A) and phase diagrams (B) of the PABS/FAD composite films, Comparing Fig. 10A and 10B, the brighter particles were thought to be FAD molecules with an average film thickness 2.2 μm. Further, Fig. 10 shows the morphology (C) and phase diagrams (D) of the PABS films, the PABS film thickness with an average size of 373 nm and the phase diagram (Fig. 10D) shows the small holes as we seen in SEM figures. When compare Fig. 10A and 10B with Fig. 10C and 10D, the flavins are strongly adsorbed as a layer with polymer film. The thickness of the PABS/FAD composite is significantly larger than that of the PABS films alone. This is an indicative of good interaction between the flavins and PABS polymer because the flavins acted as a dopant. The randomly oriented fibrils were consistently coated with polymer films. This porous morphology allows for excellent electrolyte access with less resistance. The high conductivity of PABS in the composite film increases the electrical properties of the redox processes and also provides a large surface area available for flavins intercalation.

Fig. 11 is shown the UV–vis spectrum of *p*-(ABSA) in the solution, the maximum adsorption band is located at 250 nm (Fig. 11a). The adsorption spectrum of mixed solution containing flavins and *p*-(ABSA) were shown three bands at 450, 360, and 250 nm (Fig. 11b). A conventional flavin is known to have two characteristic absorption bands at 360 and 450 nm for the oxidized form in the visible range [49]. The PABS polymer films and PABS/FAD composite films were prepared onto the ITO coated glass electrodes for investigation of native structure of flavins on the composite materials. PABS/FAD composite films on ITO glass slides showed three adsorption bands at 446, 370 and 300 nm (Fig. 11c). PABS films was shown one sharp band at 294 nm and second broad adsorption band at about 450–650 nm, these bands due to the polymer film (Fig. 11d). The spectra are dominated by two broad absorption bands at 294 nm (peak 1) and at 450–650 nm (peak 2) in aqueous solution. According to the general practice of peak assignment, peak 1 is attributed to the  $\pi$ – $\pi^*$  transition of the benzenoid moieties in the polymer linear structure or simply to the band gap of the polymer [21]. The broad band around 450–650 nm could be attributed to the intramolecular  $\pi$ – $\pi^*$  transition of benzenoid to quinoid units in the polymer structure [23]. These results suggesting that flavins in PABS films has a nearly the same as the native state of

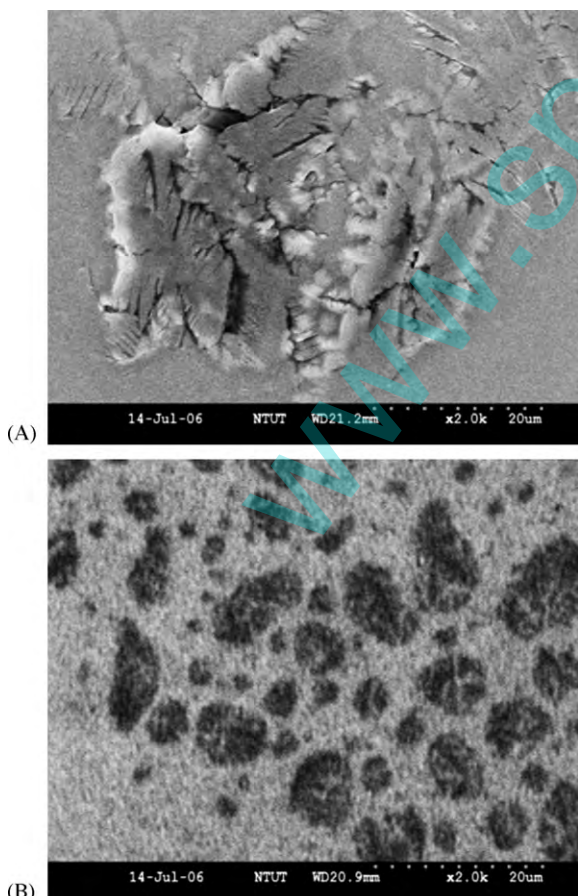


Fig. 9. SEM images of (A) PABS/FAD composite film and (B) PABS film.

flavins in solution, as previously reported by other researchers for flavins [48]

After characterizing the voltammetry of PABS/FAD/GCE in pH 6.4 phosphate buffers, electrocatalytic oxidation of NADH and reduction reaction of  $\text{NAD}^+$  in aqueous solutions was examined.

### 3.5. Effect of polymer film thickness studies

Fig. 12 shows the surface coverage versus thickness of the composite films. The PABS/FAD film was prepared using cyclic voltammetry and its thickness was measured by vary-

ing the number of cycles during polymerization, e.g., 5, 10, 15, 20, 25, 30, 35 and 40 cycles. It was interesting to observe that there was a rapid increase in surface coverage of FAD molecules and for PABS polymer up to 30 cycles, after that the surface coverage slowly tended to reach the limiting value. In the present paper, the PABS/FAD film thickness was controlled by the number of cycles during cyclic voltammetry. However, the thickness of the films was measured using AFM technique (Fig. 10A) and that was found as  $2 \pm 0.2 \mu\text{m}$  for 30 cycles in the same experimental conditions. Hence, the optimum film thickness for PABS/FAD modified electrode was  $2 \pm 0.2 \mu\text{m}$ .

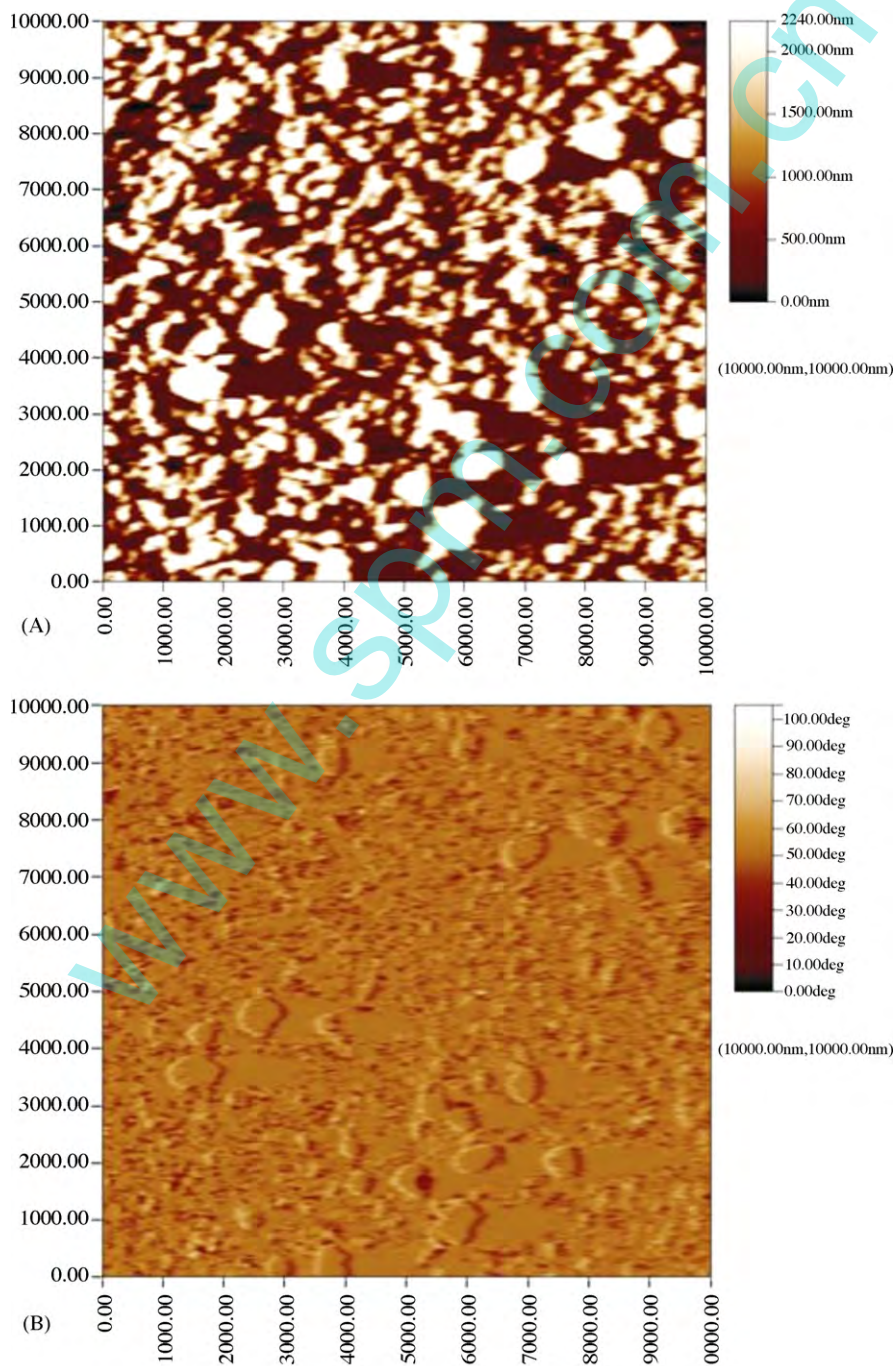


Fig. 10. The AFM morphology (A) and phase diagrams (B) of the PABS/FAD composite films; the AFM morphology (C) and phase diagrams (D) of the PABS films.

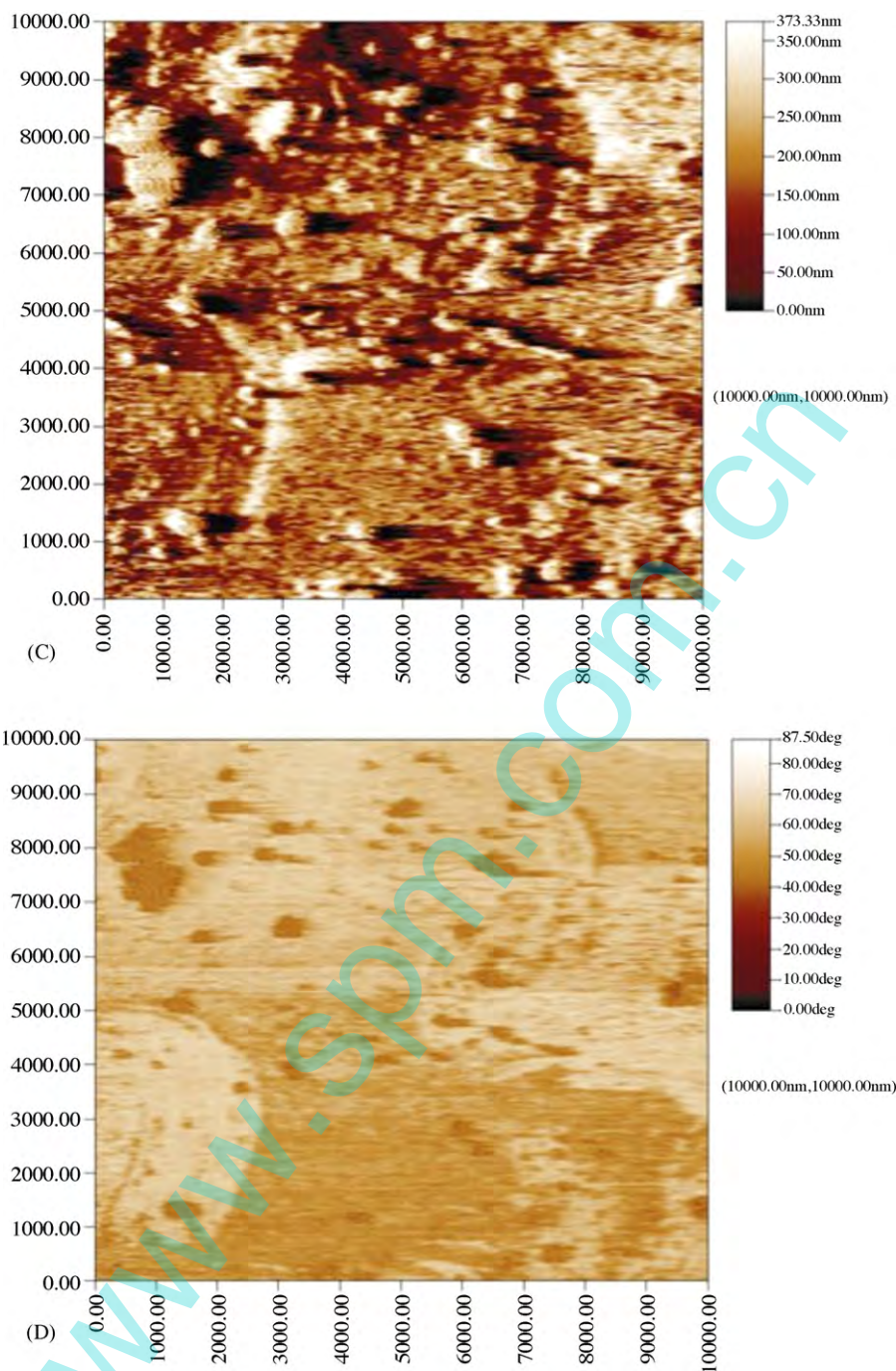


Fig. 10. (Continued).

### 3.6. Electrocatalytic oxidation of NADH

Fig. 13A details the voltammetric responses of PABS/FAD/GC working electrode (scan rate  $10 \text{ mV s}^{-1}$ ) in pH 6.4 phosphate buffer solutions towards increasing additions of NADH. Analysis of the voltammetric response at bare GCE in the presence of NADH reveals an oxidative wave about  $+0.6 \text{ V}$ . Upon the addition of NADH to the solution an increase in the oxidative peak current is observed at  $+0.20 \text{ V}$  over the entire concentration range studied, with a corresponding decrease in the reductive current at  $0.0 \text{ V}$ . This voltammetric response is entirely con-

sistent with polymer undergoing an electrocatalytic mediated reaction process. Fig. 13B details the corresponding standard addition plots obtained in the presence of various concentrations of NADH when the current was measured at  $+0.2 \text{ V}$ ; greatly enhanced signals are produced in the presence of the catalytic mediator. Analysis of this plot revealed a linear range from  $10$  to  $300 \mu\text{M}$  with a correlation coefficient of  $0.992$ . The relationship between the response current and the concentration starts to deviate slightly from the straight line at the concentrations higher than  $300 \mu\text{M}$ . The detection limit is estimated to be  $1 \mu\text{M}$  ( $S/N = 3$ ).

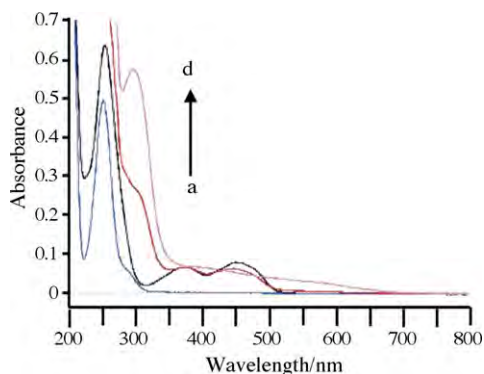


Fig. 11. UV-vis spectra of (a) *p*-(ABSA) solution, (b) mixed solution of FAD and *p*-(ABSA), (c) PABS/FAD composite films and (d) PABS films on ITO coated glass electrodes.

### 3.7. Electrocatalytic reduction of $\text{NAD}^+$

Fig. 14 shows the cyclic voltammograms of a PABS/FAD/GCE in a phosphate buffer solution in absence (curve a) and presence (curves b–d) of 20, 30 and 50  $\mu\text{M}$   $\text{NAD}^+$ . It can be seen that the reduction of  $\text{NAD}^+$  was accomplished by a clear increase in the cathodic current at a potential of  $-0.41$  V, corresponding to the catalytic reduction of  $\text{NAD}^+$ . Simultaneously, a decrease in the anodic peak current in the presence of  $\text{NAD}^+$  was also observed. No such an electrochemical reduction current was obtained at an unmodified GCE in 0.1 M phosphate buffer upon the addition of  $\text{NAD}^+$  solutions. These results indicated that  $\text{NAD}^+$  could be biocatalytically reduced at the PABS/FAD modified GCE. The FAD-mediated biocatalytical reduction of  $\text{NAD}^+$  can be presented in literature [40–42].

### 3.8. Electrocatalysis of $\text{NAD}^+/\text{NADH}$ regeneration

Electrocatalysis of  $\text{NAD}^+/\text{NADH}$  regeneration was also investigated by cyclic voltammetry at the freshly prepared PABS/FAD modified electrodes to nicotinamide adenine dinucleotide. As mentioned,  $\text{NAD}^+$  can be reduced to enzymatically active NADH using FAD as an electrocatalyst [40–42] and

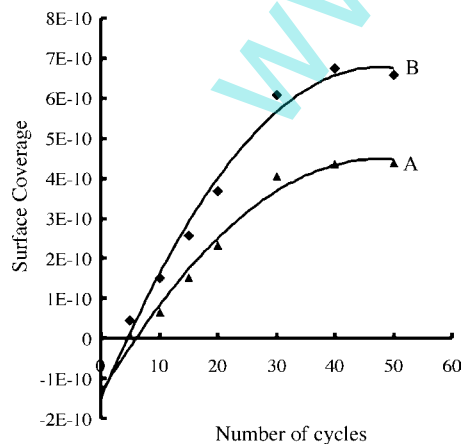


Fig. 12. Plot shows the surface coverage's vs. number of cycles of polymerization (A) FAD and (B) PABS.

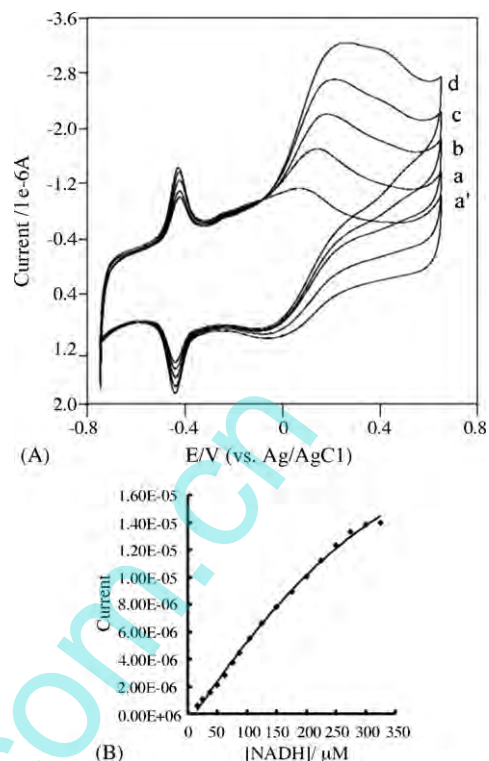


Fig. 13. (A) CVs of PABS/FAD/GCE in pH 6.4 PBS:  $\text{NADH} =$  (a') 0.0  $\mu\text{M}$ , (a) 12.5  $\mu\text{M}$ , (b) 25  $\mu\text{M}$ , (c) 37.5  $\mu\text{M}$  and (d) 50  $\mu\text{M}$ . Scan rate 10  $\text{mV s}^{-1}$ . (B) Calibration plot of  $[\text{NADH}]$  vs. peak current.

$\text{NADH}$  can be oxidized to  $\text{NAD}^+$  using PABS as an electrocatalyst, the addition of pure  $\text{NADH}$  provides the anodic (oxidation) current of polymer peak of PABS/FAD/GCE modified electrode was increased at 0.20 V (pH 6.4) (Fig. 15) where as the addition of pure  $\text{NAD}^+$  causes the cathodic (reduction) current at the FAD peak at about  $-0.41$  V. Thus, PABS/FAD modified electrode is active in both  $\text{NAD}^+$  reduction and  $\text{NADH}$  oxidation.

The anodic peak current of the PABS redox couple at a potential of about 0.20 V (versus Ag/AgCl) increased noticeably, while the cathodic peak current decreased, as the concentration

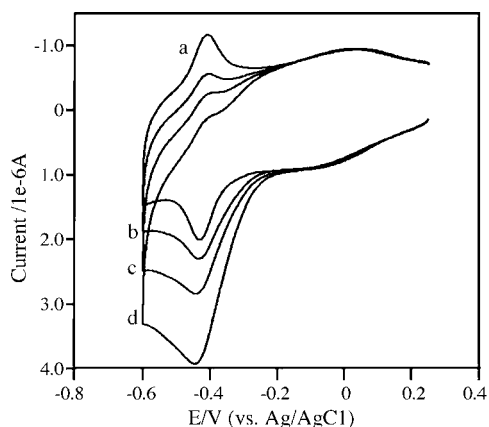


Fig. 14. CVs of PABS/FAD/GCE in pH 6.4 PBS:  $\text{NAD}^+ =$  (a) 0.0  $\mu\text{M}$ , (b) 20  $\mu\text{M}$ , (c) 30  $\mu\text{M}$  and (d) 50  $\mu\text{M}$ . Scan rate 10  $\text{mV s}^{-1}$ .

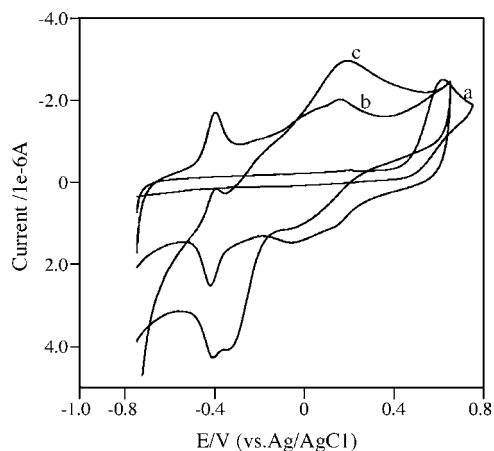


Fig. 15. CVs of PABS/FAD/GCE in pH 6.4 PBS: (b) NADH or  $\text{NAD}^+ = 0.0 \mu\text{M}$ , (c)  $50 \mu\text{M}$  NADH or  $50 \mu\text{M}$   $\text{NAD}^+$  and (a) bare GCE with  $50 \mu\text{M}$  NADH. Scan rate  $10 \text{ mV s}^{-1}$ .

of NADH increased (Fig. 15). It was indicated that the oxidation of NADH was mediated by PABS film and the  $\text{NAD}^+$  was electrocatalytically reduced by the mediated action of FAD redox couple. The reaction mechanisms when using a PABS/FAD composite film as a catalyst are described below [40–42]:

PABS (reduced form)/FAD



PABS (oxidized form)/FAD + NADH



PABS (reduced form)/FAD +  $2\text{H}^+ + 2\text{e}^-$



PABS (reduced form)/FADH<sub>2</sub> +  $\text{NAD}^+$



The stability of the PABS/FAD/GCE as discussed in Section 3.3, when compared to other modified electrode systems reported for  $\text{NAD}^+/\text{NADH}$  reversible reaction [40–42], the response of the electrode peak current reached (95%) within 2 s and the method of immobilization of flavins is simple and the enzymatic activity of flavins almost retained in the composite materials it was understood from the formal potential of flavins in solution and on the PABS film are almost same. Due to the chemical stability, electrochemical reversibility and high electron transfer rate constant of flavins on PABS modified electrodes, it can be widely used in electrocatalysis as an electron transfer mediators to shuttle electrons between analytes and substrate electrodes.

#### 4. Conclusions

We reported the synthesis and properties of composite material PABS/flavins film modified electrodes, we have applied a

novel approaches for synthesis of PABS/FAD films, first one, the adenine group of FAD molecules are positively charged in acidic solution, so we opted negatively charged PABS polymer for immobilization of flavins, the oppositely charged species are very attractive for the preparation of biosensors. Hence, the PABS/FAD composite material was very stable than other method used for immobilization of flavins. The flavins acted as a dopant in the electropolymerization process of *p*-(ABSA). SEM and AFM results indicated that the doped flavins significantly changed the morphology of PABS film and the composite film formed grainy nature. The UV–vis studies confirmed that the incorporation of the flavins in the PABS film. Finally, PABS/FAD/GCE is used to electrochemically detect NADH and  $\text{NAD}^+$ . PABS/FAD/GCE showed excellent electrocatalytic activity for the oxidation of NADH and for the reduction of  $\text{NAD}^+$ . At optimum conditions, the sensor has a fast response to NADH and a good linear response to NADH in the range from 10 to  $300 \mu\text{M}$ . The CV waves of nicotinamide adenine dinucleotide reduction-oxidation ( $\text{NAD}^+/\text{NADH}$ ) reversible reaction was also reported in physiological condition.

#### Acknowledgements

This project work financially supported by the Ministry of Education and the National Science Council of Taiwan (ROC) and we acknowledge Dr. R. Thangamuthu for suggestions and discussions on this manuscript.

#### References

- [1] A.L. Underwood, R.W. Burnett, in: A.J. Bard (Ed.), *Electroanalytical Chemistry*, Marcel Dekker, New York, 1973, p. 60.
- [2] M.M. Kamal, H. Elzanowska, M. Gaur, D. Kim, V.I. Birss, *Electrochemistry of adsorbed flavin adenine dinucleotide in acidic solutions*, *J. Electroanal. Chem.* 318 (1991) 349–361.
- [3] J. Zhang, Q. Chi, E. Wang, S. Dong, A comparative study on STM imaging and electrocatalytic activity of different surfaces modified with flavin adenine dinucleotide, *Electrochim. Acta* 40 (1995) 733–744.
- [4] Y. Wang, G. Zhu, E. Wang, Electrochemical behavior of FAD at a gold electrode studied by electrochemical quartz crystal microbalance, *Anal. Chim. Acta* 338 (1997) 97–101.
- [5] L.T. Kubota, L. Gorton, A.R. Lanzilotta, A.J. McQuillan, Electrochemical behavior of FAD and FMN immobilized on  $\text{TiO}_2$  modified carbon fibres supported by ATR-IR spectroscopy of FMN on  $\text{TiO}_2$ , *Bioelectrochem. Bioener.* 47 (1998) 39–46.
- [6] X. Jiang, Q. Xu, S.K.W. Dertinger, A.D. Stroock, T. Fu, G.M. Whitesides, A general method for patterning gradients of biomolecules on surfaces using microfluidic networks, *Anal. Chem.* 77 (2005) 2338–2347.
- [7] A. Morrin, O. Ngamna, A.J. Killard, S.E. Moulton, M.R. Smyth, G.G. Wallace, An amperometric enzyme biosensor fabricated from polyaniline nanoparticles, *Electroanalysis* 17 (2005) 423–430.
- [8] A.C. Henry, T.J. Tutt, M. Galloway, Y.Y. Davidson, C.S. McWhorter, S.A. Soper, R.L. McCarley, Surface modification of poly(methyl methacrylate) used in the fabrication of microanalytical devices, *Anal. Chem.* 72 (2000) 5331–5337.
- [9] S. Cosnier, B. Galland, C. Gondron, A. Le Pellec, Electrogeneration of biotinylated functionalized polypyrroles for the simple immobilization of enzymes, *Electroanalysis* 10 (1998) 808–813.
- [10] R.E. Ionescu, C. Gondron, L.A. Gheber, S. Cosnier, R.S. Marks, Construction of amperometric immunosensors based on the electrogeneration of a permeable biotinylated polypyrrole film, *Anal. Chem.* 76 (2004) 6808–6813.

- [11] A.I. Minett, J.N. Barisci, G.G. Wallace, Immobilisation of anti-Listeria in a polypyrrole film, *React. Funct. Polym.* 53 (2002) 217–227.
- [12] Y. Lvov, in: Y. Lvov, H. Möhwald (Eds.), *Protein Architecture: Interfacing Molecular Assemblies and Immobilisation Technology*, Marcel Dekker, New York, 2000, p. 193.
- [13] J.F. Rusling, R.J. Forster, Electrochemical catalysis with redox polymer and polyion–protein films, *J. Colloid Interface Sci.* 262 (2003) 1–15.
- [14] P. Ugo, L.M. Moretto, G.A. Mazzocchin, P. Guerriero, C.R. Martin, Electrochemical preparation and characterization of an anion–permselective composite membrane for sensor technology, *Electroanalysis* 10 (1998) 1168–1173.
- [15] Y. Okahata, T. Tsuruta, K. Ijiri, K. Ariga, Preparations of Langmuir–Blodgett films of enzyme–lipid complexes: a glucose sensor membrane, *Thin Solid Films* 180 (1989) 65–72.
- [16] D. Zhou, C.O. Too, G.G. Wallace, Synthesis and characterisation of polypyrrole/heparin composites, *React. Funct. Polym.* 39 (1999) 19–26.
- [17] V. Misoska, W.E. Price, S.F. Ralph, G.G. Wallace, N. Ogata, Synthesis, characterisation and ion transport studies on polypyrrole/deoxyribonucleic acid conducting polymer membranes, *Synth. Met.* 123 (2001) 279–286.
- [18] B. Winther-Jensen, J. Chen, K. West, G.G. Wallace, Vapor phase polymerization of pyrrole and thiophene using iron(III) sulfonates as oxidizing agents, *Macromolecules* 37 (2004) 5930–5935.
- [19] B. Winther-Jensen, J. Chen, K. West, G.G. Wallace, ‘Stuffed’ conducting polymers, *Polymer* 46 (13) (2005) 4664–4669.
- [20] J. Chen, B. Winther-Jensen, C. Lynam, O. Ngamna, S. Moulton, W. Zhang, G.G. Wallace, A simple means to immobilize enzyme into conducting polymers via entrapment, *Electrochem. Solid-State Lett.* 9 (7) (2006) H68–H70.
- [21] Y. Sahin, K. Pekmez, A. Yildiz, Electrochemical preparation of soluble sulfonated polymers and aniline copolymers of aniline sulfonic acids in dimethylsulfoxide, *J. Appl. Polym. Sci.* 90 (2003) 2163–2169.
- [22] J. Yue, A.J. Epstein, Synthesis of self-doped conducting polyaniline, *J. Am. Chem. Soc.* 112 (1990) 2800–2801.
- [23] J. Yue, Z.H. Wang, K.R. Cromack, A.J. Epstein, A.G. MacDiarmid, Effect of sulfonic acid group on polyaniline backbone, *J. Am. Chem. Soc.* 113 (1991) 2665–2671.
- [24] J. Yue, G. Gordon, A.J. Epstein, Comparison of different synthetic routes for sulphonation of polyaniline, *Polymer* 33 (1992) 4410–4418.
- [25] C. Barbero, M.C. Miras, R. Koetz, O. Haas, Comparative study of the ion exchange and electrochemical properties of sulfonated polyaniline (SPAN) and polyaniline (PANI), *Synth. Met.* 55 (1993) 1539–1544.
- [26] M. Ferreira, M.F. Rubner, Molecular-level processing of conjugated polymers. 1. Layer-by-layer manipulation of conjugated polyions, *Macromolecules* 28 (1995) 7107–7114.
- [27] A.G. MacDiarmid, A.J. Epstein, The concept of secondary doping as applied to polyaniline, *Synth. Met.* 65 (1994) 103–116.
- [28] Y. Cao, A.J. Heeger, Magnetic susceptibility of polyaniline in solution in non-polar organic solvents and in polyblends in poly(methyl methacrylate), *Synth. Met.* 52 (1993) 193–200.
- [29] S. Shimizu, T. Saitoh, M. Uzawa, M. Yuasa, K. Yano, T. Maruyama, K. Watanabe, Synthesis and applications of sulfonated polyaniline, *Synth. Met.* 85 (1997) 1337–1338.
- [30] J. Yue, A.J. Epstein, Z. Zhong, P.K. Gallogher, A.G. MacDiarmid, Thermal stabilities of polyanilines, *Synth. Met.* 41 (1991) 765–768.
- [31] A.A. Karyakin, Y.N. Ivanova, E.E. Karyakina, Equilibrium (NAD<sup>+</sup>/NADH) potential on poly(Neutral Red) modified electrode, *Electrochem. Commun.* 5 (2003) 677–680.
- [32] D.C. Tse, T. Kuwana, Electrocatalysis of dihydronicotinamide adenosine diphosphate with quinones and modified quinone electrodes, *Anal. Chem.* 50 (1978) 1315–1318.
- [33] H. Huck, H.-L. Schmidt, Chloranil as a catalyst for the electrochemical oxidation of NADH to NAD<sup>+</sup>, *Angew. Chem. Int. Ed. Engl.* 20 (1981) 402–403.
- [34] A. Malinauskas, J.J. Kulys, Alcohol, lactate and glutamate sensors based on oxidoreductases with regeneration of nicotinamide adenine dinucleotide, *Anal. Chim. Acta* 98 (1978) 31–37.
- [35] L. Gorton, Chemically modified electrodes for the electrocatalytic oxidation of nicotinamide coenzymes, *J. Chem. Soc., Faraday Trans. 1* 182 (4) (1986) 1245–1258.
- [36] P.N. Bartlett, E.N.K. Wallace, The oxidation of  $\beta$ -nicotinamide adenine dinucleotide (NADH) at poly(aniline)-coated electrodes. Part II. Kinetics of reaction at poly(aniline)–poly(styrenesulfonate) composites, *J. Electroanal. Chem.* 486 (2000) 23–31.
- [37] A. Torstensson, L. Gorton, Catalytic oxidation of NADH by surface-modified graphite electrodes, *J. Electroanal. Chem.* 130 (1981) 199–207.
- [38] B. Persson, L. Gorton, A comparative study of some 3,7-diaminophenoxazine derivatives and related compounds for electrocatalytic oxidation of NADH, *J. Electroanal. Chem.* 292 (1990) 115–138.
- [39] R. Weinkamp, E. Steckhan, Indirect electrochemical regeneration of NADH by a bipyridinerhodium(I) complex as electron-transfer agent, *Angew. Chem. Int. Ed. Engl.* 21 (1982) 782–783.
- [40] K.-C. Lin, S.-M. Chen, Reversible cyclic voltammetry of the NADH/NAD<sup>+</sup> redox system on hybrid poly(luminol)/FAD film modified electrodes, *J. Electroanal. Chem.* 589 (2006) 52–59.
- [41] S.M. Chen, M.-I. Liu, Electrocatalytic properties of NDGA and NDGA/FAD hybrid film modified electrodes for NADH/NAD<sup>+</sup> redox reaction, *Electrochim. Acta* 51 (2006) 4744–4753.
- [42] K.-C. Lin, S.-M. Chen, Characterization of hybrid poly(acriflavine)/FAD films and their electrocatalytic properties with NAD<sup>+</sup> and NADH, *J. Electrochem. Soc.* 153 (5) (2006) D91–D98.
- [43] G. Jin, Y. Zhang, W. Cheng, Poly(*p*-aminobenzene sulfonic acid)-modified glassy carbon electrode for simultaneous detection of dopamine and ascorbic acid, *Sens. Actuators B* 107 (2005) 528–534.
- [44] E. Lavion, General expression of the linear potential sweep voltammogram in the case of diffusionless electrochemical systems, *J. Electroanal. Chem.* 101 (1979) 19–28.
- [45] E. Laviron, Adsorption, autoinhibition and autocatalysis in polarography and in linear potential sweep voltammetry, *J. Electroanal. Chem.* 52 (1974) 355–393.
- [46] V.I. Birss, H. Elzanowska, R.A. Turner, The electrochemical behavior of flavin adenine dinucleotide in neutral solutions, *Can. J. Chem.* 66 (1988) 86–96.
- [47] V.I. Birss, A.S. Hinman, C.E.W. Garvey, J. Segal, *In situ* FTIR thin-layer reflectance spectroscopy of flavin adenine dinucleotide at a mercury/gold electrode, *Electrochim. Acta* 39 (1994) 2449–2454.
- [48] V.I. Birss, S. Guha-Thakurta, C.E. McGarvey, S. Quach, P. Vanysek, An electrochemical study of the photolysis of adsorbed flavins, *J. Electroanal. Chem.* 423 (1997) 13–21.
- [49] M. Yamashita, S.S. Rosatto, L. Kubota, Electrochemical comparative study of Riboflavin, FMN and FAD immobilized on the silica gel modified with zirconium oxide, *J. Braz. Chem. Soc.* 13 (2002) 635–641.
- [50] R. Garjonyte, A. Malinauskas, L. Gorton, Investigation of electrochemical properties of FMN and FAD adsorbed on titanium electrode, *Bioelectrochemistry* 61 (2003) 39–49.
- [51] F. Fusalba, P. Gouérec, D. Villers, D. Bélanger, Electrochemical characterization of polyaniline in nonaqueous electrolyte and its evaluation as electrode material for electrochemical supercapacitors, *J. Electrochem. Soc.* 148 (2001) A1–A6.

## Biographies

**S. Ashok Kumar** obtained his undergraduate degree in chemistry in 2000 from University of Madras in Chennai, India. Then he graduated with his MSc in Industrial chemistry from A.V.V. M Sri Pushpam College, Bharathidasan University in 2002, Tamilnadu, and then he obtained his MPhil degree in Analytical Chemistry from University of Madras in 2004. At present he is PhD student at Department of Chemical Engineering and Biotechnology, National Taipei University of Technology, Taipei, Taiwan. His current research involves mainly bioelectrochemistry and development of biosensors based on conducting polymers for the application of real samples.

**Shen-Ming Chen** was born in Chunghua, Taiwan, in 1957. He received his BSc degree in chemistry in 1980 from National Kaohsiung Normal Univer-

city, Kaohsiung, Taiwan. He received his MSc and PhD degrees in chemistry in 1983 and 1991 from National Taiwan University, Taipei, Taiwan. He was a visiting postdoctoral fellow with the Institute of Inorganic Chemistry, Friedrich-Alexander University Erlangen-Nuremberg, Germany in 1997. He had been an associate professor of Department of Chemical Engineering, National Taipei

Institute of Technology, Taipei, Taiwan from 1991 to 1997. Since August 1997, he has been a full professor of Department of Chemical Engineering and Biotechnology, National Taipei University of Technology, Taipei, Taiwan. His research interest includes bioelectrochemistry, biosensors and drug analysis.

[www.spm.com.cn](http://www.spm.com.cn)